*Manuscript
Click here to view linked References

Quantification of the Performance of Iterative and Non-Iterative Computational Methods of Locating Partial Discharges Using RF Measurement Techniques

Othmane El Mountassir [1*], Brian G Stewart [2], Alistair J Reid [3] and Scott G McMeekin [4]

1 Offshore Renewable Energy Catapult, 121 George Street, Glasgow G1 1RD, UK
2 Department of Electronic and Electrical Engineering, University of Strathclyde, 204 George Street, Glasgow G1 1XW, UK
3 School of Engineering, Cardiff University, The Parade, Cardiff CF24 3AA, UK
4 Institute for Sustainable Engineering & Technology, Glasgow Caledonian University, 70 Cowcaddens Road, Glasgow G4 0BA, UK

Abstract

Partial discharge (PD) is an electrical discharge phenomenon that occurs when the insulation material of high voltage equipment is subjected to high electric field stress. Its occurrence can be an indication of incipient failure within power equipment such as power transformers, underground transmission cable or switchgear. Radio frequency measurement methods can be used to detect and locate discharge sources by measuring the propagated electromagnetic wave arising as a result of ionic charge acceleration. An array of at least four receiving antennas may be employed to detect any radiated discharge signals, then the three dimensional position of the discharge source can be calculated using different algorithms. These algorithms fall into two categories; iterative or non-iterative.

This paper evaluates, through simulation, the location performance of an iterative method (the standard least squares method) and a non-iterative method (the Bancroft algorithm). Simulations were carried out using (i) a “Y” shaped antenna array and (ii) a square shaped antenna array, each consisting of a four-antennas. The results show that PD location accuracy is influenced by the algorithm’s error bound, the number of iterations and the initial values for the iterative algorithms, as well as the antenna arrangement for both the non-iterative and iterative algorithms. Furthermore, this

research proposes a novel approach for selecting adequate error bounds and number of iterations using results of the non-iterative method, thus solving some of the iterative method dependencies.

Keywords: Partial discharges; Iterative algorithms; Non-Iterative algorithms; Radio Frequency; Fault location; Time difference of arrival.

1 Introduction

Radio frequency (RF) measurement technique using receiving antennas can be used to detect the radiated energy from PD sources or any other electrical discharge activities, subsequently facilitating the discharge source triangulation. Using a receiving antenna array, which may be arranged in various forms, the time differences of arrival (TDOA) between received signals on each of the respective antennas allows the 3 dimensional position of the electrical discharge source to be deduced by processing of the TDOA values through iterative or non-iterative location algorithms. The location of partial discharges using emitted RF techniques in HV equipment has been widely investigated [1-5]. Research in this area has been carried out on cables [6-9], gas and air insulated switchgears [10-14] and transformers [15-17]. PD location in cables, and to a degree in gas-insulated substation (GIS), is a two-dimensional problem, while internal localisation within power transformers and localisation in three dimensions in wide-area HV substations requires robust computation algorithms [1].

There are two types of computational algorithm which can be used to locate partial discharges in three dimensions; (i) iterative methods and (ii) non-iterative methods. In this study, a non-iterative method was selected due to the large success of these methods in Global Positioning System (GPS) applications such as navigation and location systems. The choice of an iterative method was mainly due their efficiency in solving nonlinear problems involving large number of variables.

The iterative methods give an approximate solution to nonlinear equations based on a number of iterations and starting with an initial value, which is improved at each iteration by an error bound until a converged solution is found or until a maximum number of iterations is reached. Taylor expansion and Newton-Raphson techniques are common iterative methods that can be used to solve the equations of nonlinear systems.

These methods have been used in different studies to locate PD [1, 18-19]. The study in [18] highlighted that the performance of the Taylor expansion method depends on the accuracy of the initial values and the number of sensors, whereas the study by [1] showed that the Newton-Raphson method successfully locates PD and that the location accuracy depends on the arrangement of antennas. Study [19] also used the Newton-Raphson method to locate PD and found that in some cases the algorithm did not provide a converged solution. It indicated that a solution called the "grid search method" which consists of using a range of values within a grid as initial values to determine a converged solution helped improve accuracy. Despite the fact that these studies highlighted the success of these iterative methods to locate discharges activities within a reasonable margin of error, a limited number of published studies have attempted to evaluate fully the performance of non-iterative and iterative methods in their ability to locate accurately the position of electrical discharge sources.

In order to evaluate the performance of iterative and non-iterative algorithms, the present study investigates through simulation the location performance of a well-established iterative method; the standard least squares (SLS) method, and a non-iterative method; the Bancroft algorithm [22]. Two antenna array configurations (Y and square shape), both consisting of 4 antenna positions were chosen for the investigations reported herein evaluating the performance of the respective location algorithms. The square and 'Y' array configurations are commonly used and were selected since they have been used in previous studies [1, 4] to investigate electromagnetic (EM) wave propagation PD sources.

The paper is structured as follows: The mathematical formulation of the SLS and Bancroft location algorithms are presented in Section II; Section III presents the methodologies used in the present study; Section IV presents the results of PD location

studies using the SLS and Bancroft algorithms respectively (in each case two different antenna arrangements were investigated). For simplification, the simulated PD location data points refer to any electrical discharge source emitting EM wave radiation; Section V compares the characteristics of both the iterative and non-iterative algorithms used; Section VI proposes a new approach to select adequate error bounds and number of iterations using results of the non-iterative methods; Section VII summarises the findings of the study.

2 Formulation of the SLS and Bancroft Algorithms

A minimum of four spatially separated antennas may be used to triangulate the location of a PD event in 3 dimensions using RF methods (Figure 1). Knowing the grid coordinates of each antenna in the array then allows the propagation time from the PD source to the respective antennas to be calculated using the basic formula $D = v.t$, Where D is distance, v is propagation velocity and t is propagation time. This technique, commonly referred to as 'triangulation', is described by Equation (1):

$$(x - x_i)^2 + (y - y_i)^2 + (z - z_i)^2 = (v_e \cdot t_i)^2 \quad (1)$$

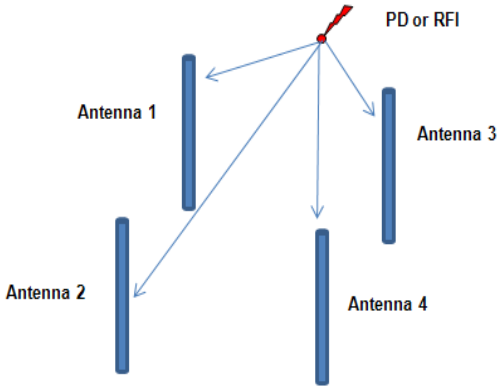

Figure 1: Basic configuration of a typical RF PD location setup.

Where (x_i, y_i, z_i) are the coordinates of the i^{th} antenna in Cartesian space, (x, y, z) represent the true coordinates of the PD event, v_e is the speed of light $(3 \times 10^8$ m/s$)$ and t_i

represents the 'time-of-flight' of the propagating PD signal from its source to the i^{th} antenna. It should be noted that since the study is a simulation based investigation, the speed of light was considered to be in a vacuum and that this value changes depending on the insulating material.

Let the time-of-flight from the PD source to antenna A_1 be T and the time-difference-of-arrival between antennas A_1 and A_n ($n = 2, 3, 4$) be τ_{1n}. Equation (1) now expands into the following four formulae [20]:

$$\begin{aligned}
&(x-x_1)^2+(y-y_1)^2+(z-z_1)^2=(v_e\cdot T)^2\\
&(x-x_2)^2+(y-y_2)^2+(z-z_2)^2=\left(v_e\cdot(T+\tau_{12})\right)^2\\
&(x-x_3)^2+(y-y_3)^2+(z-z_3)^2=\left(v_e\cdot(T+\tau_{13})\right)^2\\
&(x-x_4)^2+(y-y_4)^2+(z-z_4)^2=\left(v_e\cdot(T+\tau_{14})\right)^2
\end{aligned} \tag{2}$$

2.1 Standard Least Squares (SLS) algorithm

Using on the non-linear equations in (2), the position of a PD source (x, y, z) can be computed using the least squares method given in Equation (3).

$$S(X)=\sum_{i=1}^{N}(Y_i(X))^2 \tag{3}$$

In least squares, the standard definition of $Y_i(X)$ is given in Equation (4). Based on the definition of $Y_i(X)$, the least squares method minimises the sum of the square of the residuals.

$$Y_i(X)=\sqrt{(x-x_i)^2+(y-y_i)^2+(z-z_i)^2}-(v_e*(T+\tau_{1i})) \tag{4}$$

Since the aim is to compute the values of x, y and z which minimise $S(X)$, the partial derivative of $S(X)$ with respect to x, y and z is calculated with the equation set equal to 0 as shown in Equation (5):

$$\frac{\partial S}{\partial x}=0,\ \frac{\partial S}{\partial y}=0,\ \frac{\partial S}{\partial z}=0 \text{ and } \frac{\partial S}{\partial T}=0. \tag{5}$$

Substituting p to represent x, y or z, the iterative solution for each coordinate and for T becomes:

$$p = \frac{1}{N}\sum_{i=1}^{N} p_i + \frac{1}{N}\sum_{i=1}^{N} \frac{(p - p_i)(T + \tau_{1i})v_e}{\sqrt{(x - x_i)^2 + (y - y_i)^2 + (z - z_i)^2}} \tag{6}$$

$$T = \frac{\sum_{i=1}^{N} \sqrt{(x - x_i)^2 + (y - y_i)^2 + (z - z_i)^2}}{\sum_{i=1}^{N} v_e} - \frac{1}{N}\sum_{i=1}^{N} \tau_{1i} \tag{7}$$

Where N is the number of antennae and τ_{1i} is the TDOA between a signal measured by the i^{th} antenna and by antenna 1. For chosen initial conditions, the formulae derived above may be applied iteratively until solutions for x, y and z are converged upon, given a defined error bound and an upper limit on the number of iterations [4, 21].

2.2 Bancroft algorithm

Developed by Bancroft [22], this algorithm was derived for application to global positioning system (GPS) location. Bancroft's algorithm makes use of the Lorenz inner product for time-space vectors, which is defined considering u and w vectors of the form:

$$u = \begin{bmatrix} x_u \\ y_u \\ z_u \\ v * t_u \end{bmatrix}, \quad w = \begin{bmatrix} x_w \\ y_w \\ z_w \\ v * t_w \end{bmatrix} \tag{8}$$

Where x, y and z are the coordinates of the two vectors u and w, v is a constant which represent the speed of light, and t is time. The Lorenz inner product of u and w is defined as:

$$\langle u, w \rangle = x_u x_w + y_u y_w + z_u z_w - v^2 t_u t_w \tag{9}$$

Assuming there are four antennas located at (x_i, y_i, z_i), with the associated time of arrival (TOA) as t_i, where $i = 1, 2, 3, 4$ and the PD source is located at (x, y, z) and has a time of emission (TOE) t. This can presented as:

$$s_i = \begin{bmatrix} x_i \\ y_i \\ z_i \\ v*t_i \end{bmatrix} \quad , \qquad s = \begin{bmatrix} x \\ y \\ z \\ v*t \end{bmatrix} \tag{10}$$

Each TOA measurement may be expressed as:

$$(x - x_i)^2 + (y - y_i)^2 + (z - z_i)^2 = v^2*(t - t_i)^2 \tag{11}$$

Which is equivalent to:

$$2(xx_i + yy_i + zz_i - v^2 t_i t) = x^2 + y^2 + z^2 - v^2 t^2 + x_i^{\,2} + y_i^{\,2} + z_i^{\,2} - v^2 t^2{}_i \tag{12}$$

or, in vector-matrix form:

$$2As = \lambda I + b \tag{13}$$

Where

$s = \begin{bmatrix} x \\ y \\ z \\ v*t \end{bmatrix}$, are the coordinates of interest

$$A = \begin{bmatrix} x_1 & y_1 & z_1 & -vt_1 \\ x_2 & y_2 & z_2 & -vt_2 \\ x_3 & y_3 & z_3 & -vt_3 \\ x_4 & y_4 & z_4 & -vt_4 \end{bmatrix}, \ \lambda = \langle s, s \rangle = x^2 + y^2 + z^2 - v^2 t^2 \ \text{ and } \ 1 = \begin{bmatrix} 1 \\ 1 \\ 1 \\ 1 \end{bmatrix}$$

$$b = \begin{bmatrix} \langle s_1, s_1 \rangle \\ \langle s_2, s_2 \rangle \\ \langle s_3, s_3 \rangle \\ \langle s_4, s_4 \rangle \end{bmatrix} = \begin{bmatrix} x_1^{\,2} + y_1^{\,2} + z_1^{\,2} - v^2 t_1^{\,2} \\ x_2^{\,2} + y_2^{\,2} + z_2^{\,2} - v^2 t_2^{\,2} \\ x_3^{\,2} + y_3^{\,2} + z_3^{\,2} - v^2 t_3^{\,2} \\ x_4^{\,2} + y_4^{\,2} + z_4^{\,2} - v^2 t_4^{\,2} \end{bmatrix}$$

Based on equation (13), which relates $\boldsymbol{s}$ to its Lorenzian norm λ, this can be rewritten as:

$$s = \frac{1}{2}\lambda A^{-1} 1 + \frac{1}{2} A^{-1} b \qquad \text{or} \qquad s = \lambda d + e \tag{14}$$

Where

$$d = \frac{1}{2} A^{-1} 1 = \begin{bmatrix} x_d & y_d & z_d & vt_d \end{bmatrix}^T, \qquad e = \frac{1}{2} A^{-1} b = \begin{bmatrix} x_e & y_e & z_e & vt_e \end{bmatrix}^T$$

Taking the Lorenzian norm of both sides of equation (14) results in a quadratic equation in λ, i.e.

$$\lambda = \langle d, d \rangle \lambda^2 + 2\langle d, e \rangle \lambda + \langle e, e \rangle \quad \text{or} \qquad \alpha\lambda^2 + \beta\lambda + \gamma = 0 \tag{15}$$

Where

$$\alpha = \langle d, d \rangle = x_d{}^2 + y_d{}^2 + z_d{}^2 - v^2 t_d{}^2$$

$$\beta = 2\langle d, e \rangle - 1 = 2x_d x_e + 2y_d y_e + 2z_d z_e - 2vt_d t_e - 1$$

$$\gamma = \langle e, e \rangle = x_e{}^2 + y_e{}^2 + z_e{}^2 - v^2 t_e{}^2$$

Solving the quadratic equation (15) results in two solutions of λ when $\alpha \neq 0$ and the possible PD solutions are located either at:

$$s_1 = \lambda_1 d + e = \begin{bmatrix} x \\ y \\ z \\ vt \end{bmatrix}, \text{ or } \quad s_2 = \lambda_2 d + e = \begin{bmatrix} x \\ y \\ z \\ vt \end{bmatrix} \tag{16}$$

In GPS technology, the selection of a valid solution is based on clock synchronisation and thus the solution with the lowest time offset (presented by *vt* in both s_1 and s_2 vector) is considered to be a correct solution.

3 Methodology

The authors have developed a software platform in MATLAB that performs simulation and localisation for an array of PD source positions (a grid of 64 PD positions were simulated, as depicted in Figure 2). The positions were selected arbitrarily on a Cartesian grid as PD sources can occur anywhere within the insulation system of HV assets. Figure 2 also shows the configuration of the antenna arrays (triangular symbols). Simulations have been performed on both the Y shaped (Figure 2a) and the square

shaped array (Figure 2b). Table 1 presents the grid coordinates of each antenna. These antenna arrangement arrays were considered in a way to enable an easy setting of these equipment when measurements are carried out in a real site environment, although antenna arrays will generally be placed away from substation equipment to respect distance clearances.

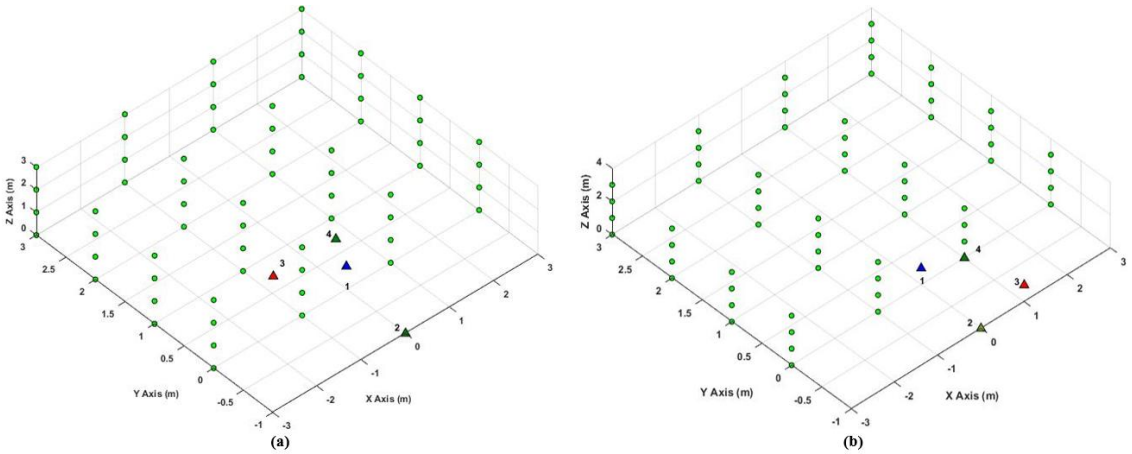

Figure 2: Simulation geometry showing PD locations (green spheres) and antenna locations (triangles) for the two array configurations (a) Y shaped array and (b) Square shaped array

Table 1: Coordinates of the antenna arrays within the simulation grid

Antenna number	***Y shaped array***			***Square shaped array***		
	x (m)	***y (m)***	***z (m)***	***x (m)***	***y (m)***	***z (m)***
1	0	0	1	0	0	1
2	0	-1	0	0	-1	0
3	$-1/\sqrt{2}$	$1/\sqrt{2}$	0	1	-1	1
4	$1/\sqrt{2}$	$1/\sqrt{2}$	0	1	0	0

In the case of the Y shaped array, the respective antennae were mutually separated by a distance of 1 m, with 3 of the antennas positioned on the horizontal plane and a single central antenna elevated by 1m in the vertical plane. In the case of the square array, antenna positions were spaced apart by 1m horizontally. Diametrically opposite antennas were offset by 1 m in the *z* axis. The number of 3D PD locations was chosen based on processing time considerations. Simulated PD locations fill a defined volume

that surrounds the antenna arrays. PD positions lie along the *x*-axis from 3 m to 3 m at intervals of 2 m, along the *y*-axis from 0 m to 3 m at intervals of 1 m and along the *z*-axis from 0 m to 3 m also at intervals of 1 m. The range of the simulated PD positions was selected so that precise appreciation of the location performance of the iterative and non-iterative algorithms was provided.

The TDOAs of the simulated PD positions were obtained using Equation 8, where (*x, y, z*) represent the coordinates of the simulated PD position and (x_i, y_i, z_i) the coordinates of the four antennas (*1, 2, 3* and *4*). The iterative algorithm (SLS) was applied and its performance evaluated, with the initial values for (*x, y, z*) set to (*0, 0, 0*). Within the iteration method, error bounds were varied from 10^{-3} down to 10^{-13} with an additional error bound defined for the time iteration and having a value of 10^{-8}. The error bound can be defined as the incremental limit between consecutive iterations of the algorithm that produces a converged solution, thus determining the accuracy of the iterative solutions. The accuracy of the iterative method has been evaluated in terms of accuracy by comparing the difference in distance *d* between the iterated solution to the PD location and the actual PD location. Four categories of location accuracy were defined:

- Very good accuracy: $d \leq 1$ cm
- Good accuracy: 1 cm $< d \leq 50$ cm
- Poor accuracy: 50 cm $< d \leq 1$ m
- Very poor accuracy: $d > 1$ m

Moreover, the computational efficiencies of the algorithms were assessed by calculating the total number of iterations used to achieve converge on the stipulated error bound accuracy. This was repeated for both antenna array configurations.

Regarding the non-iterative methods, these are well known for providing precise estimates of the location when they are provided with accurate TDOAs [23]. In GPS,

there are always uncertainties in TDOA measurements and satellite positions. These inaccuracies give rise to random errors of the emitter location. However, the location accuracy can be improved by solving the clock error of the receiver [24], by using pseudo-range observations [22] or by limiting the TOA range based on the altitude of the GPS satellites [25].

Determining the location of PD using non-iterative methods is a more difficult process, as PD sources do not provide a time of emission to establish synchronisation with the receiving sensors. In this context, results sections of the non-iterative algorithms evaluate the output of the two solutions provided by these algorithms as the simulated PD have accurate theoretical TOAs based on equation (1). The accuracy of the non-iterative algorithms have been evaluated in terms of PD location by determining the difference between the calculated PD solutions (i.e. two roots solutions provided by the quadratic equations of the algorithms) and the simulated positions. Two categories were defined:

- Correct location: difference between calculated PD solution and simulated PD position equal to 0.
- Incorrect location: difference between calculated PD solution and simulated PD position not equal to 0.

4 Location Performance of the Algorithms

The following sections present the location results of the SLS and Bancroft algorithms using the two different antenna arrangements. The location results will be discussed in terms of location accuracy for both iterative and non-iterative methods and also the number of iterations for the SLS algorithm.

4.1 Standard Least Squares (SLS) algorithm

4.1.1 Y-shaped array

To ensure converged solutions for all 64 simulated PD locations, sufficient iterations were applied to the SLS algorithm for various error bounds. For the specified error bounds, Figure 3 plots the number of converged PD location solutions within each of the four accuracy categories defined above. It can be seen that the number of PD sources located with very poor accuracy (greater than 1m from the simulated locations) saw a marked decrease as the error bound reduced, allowing improvement in the intermediate distances and convergence towards highly accurate positions (i.e 34 solutions less than 1 cm from the true PD source position). As the error bound was reduced further, no additional improvement was seen. This result demonstrates that location accuracy is influenced not only by the physical arrangement of the antennas, the TDOA of the signals and the accuracy of the digital sampling hardware, but also on the error bound set within the location algorithm.

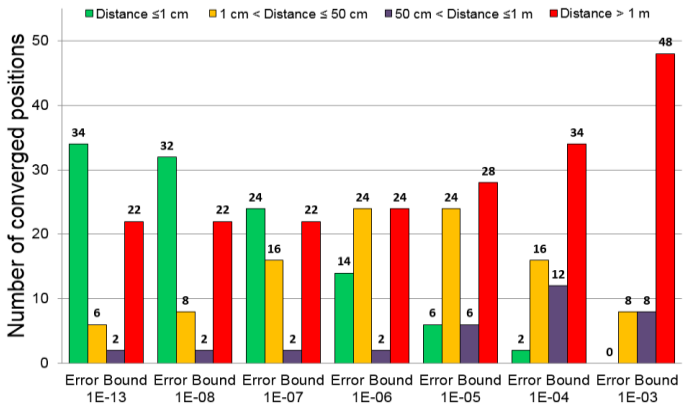

Figure 3: Number of converged PD position solutions as a function of location accuracy and error bound for simulations on the Y-shaped antenna array (SLS)

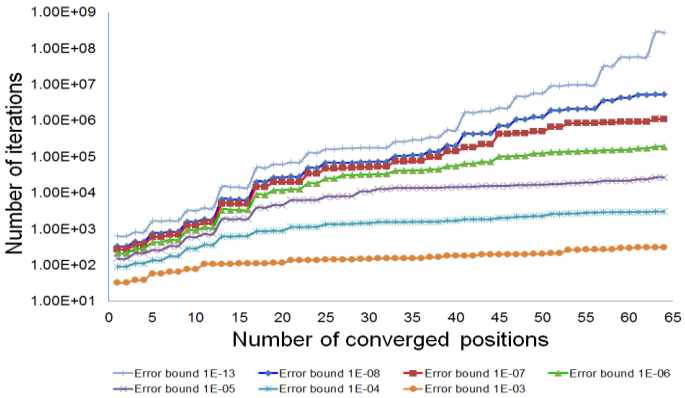

Figure 4: Results of simulations on the Y-shaped antenna array showing number of iterations vs. number of converged PD positions for various error bounds (SLS).

Figure 4 plots the total number of iterations needed for solutions to converge on all 64 PD locations for the seven error bounds under consideration. This result demonstrates the relationship between the number of iterations and the error bound, with the former increasing significantly from a few hundred to hundreds of millions as the error bound decreases. Such a large number of iterations has the consequence of increasing computational time from a few seconds to several hours using a standard desktop machine (computation of these results were carried out using an Intel Q6600 Core2 Quad 2.4 GHz Processor). Extended computing times would be impractical if location were required in real-time or close to real-time.

The percentage of PD sources pinpointed within the defined accuracy limits is shown in Table 2 together with the number of iterations performed for each respective error bound. It is clear from Table 2 that the location accuracy improves as the error bound decreases. Consequently, the iterative steps accumulate in number. Additionally, using the lowest error bound i.e. 10^{-13}, which was found to be the best possible accuracy for this arrangement, the number of PDs located at more than 1 m from the simulated positions was found to be slightly high. This is due to the spatial separation between the different antennas and the antenna arrangement as further results using the square antenna arrangement shows improved location accuracy.

Table 2: Results of SLS algorithm showing percentage of solutions converging within the defined location accuracy limits for the Y-shaped antenna array.

Error Bound	d ≤ 1 cm	1 cm < d ≤50 cm	50 cm < d ≤1 m	d > 1 m	No. of Iterations
10^{-13}	53.1%	9.4%	3.1%	34.4%	275740268
10^{-08}	50.0%	12.5%	3.1%	34.4%	5371396
10^{-07}	37.5%	25%	3.1%	34.4%	1104646
10^{-06}	21.9%	37.5%	3.1%	37.5%	194065
10^{-05}	9.4%	37.5%	9.4%	43.8%	27325
10^{-04}	3.1%	25%	18.8%	53.1%	3164
10^{-03}	0.0%	12.5%	12.5%	75.0%	315

Table 3: Results of SLS algorithm showing percentage of solutions converging within the defined location accuracy limits for the square-shaped antenna array.

Error Bound	d ≤ 1 cm	1 cm < d ≤50 cm	50 cm < d ≤1 m	d > 1 m	No. of Iterations
10^{-13}	95.3%	0%	0%	4.7%	2212354990
10^{-08}	84.4%	10.9%	0%	4.7%	11755016
10^{-07}	67.2%	26.6%	1.6%	4.7%	1727533
10^{-06}	29.7%	57.8%	6.3%	6.3%	243296
10^{-05}	7.8%	60.9%	15.6%	15.6%	55905
10^{-04}	1.6%	34.4%	15.6%	48.4%	4140
10^{-03}	0%	18.8%	15.6%	65.5%	263

4.1.2 Square-shaped array

The results obtained using SLS with the square antenna array proved similar to those obtained previously with regards to the accuracy and number of iterations (See Figure 5 and Figure 6). With an error bound of 10^{-03}, 42 PD positions were located with very poor accuracy (metres from their true position). The number of PD located > 1 m from the simulated positions was reduced significantly as the error bound became smaller, allowing the intermediate distances to improve and solutions to converge towards very accurate locations of less than 1 cm from the true PD source position. However, Table 3 shows a considerable improvement of the location accuracy. At an error bound of 10^{-13}, *95.3%* of iterated PD positions were to within an accuracy of less than 1 cm. Whereas, in the case of the Y-shaped array configuration, only *53.1%* of PD were located to within the same accuracy at the same error bound. The 3 remaining PD positions

located at a distance of > 1 m did not show any further improvement despite further reduction in the error bound. The non-location of these PD positions was mainly due to the applied initial value (*0, 0, 0*) since, after replacing those initial values by the actual true value of the PD locations, calculation provided a correct solution.

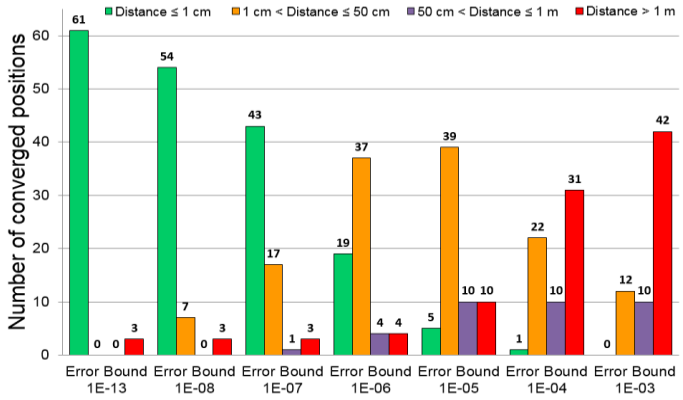

Figure 5: Number of converged positions as a function of both location accuracy and error bound for square shaped arrangement (SLS)

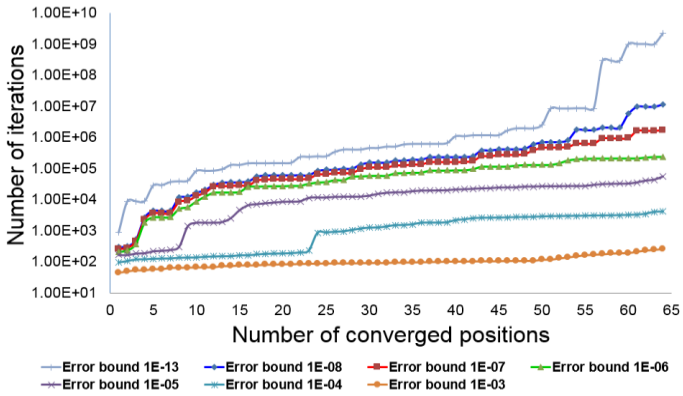

Figure 6: Results of simulations on the square-shaped antenna array showing number of iterations vs. number of converged PD positions for various error bounds (SLS).

4.1.3 Discussion

As shown in Table 2 and Table 3, which present respectively the effectiveness of the Y and square shape arrays to locate PD occurring at each of the 64 grid positions, it can be seen that in the case of the square array, *95.3%* of the converged solutions locate PD to within 1 cm of their true position at an error bound of 10^{-13}. In contrast, the Y shaped

array, is only capable of locating *53.1%* of the PDs to within than 1 cm of their true position at the same error bound, which represents the best possible accuracy for this arrangement in the present study. These results show that in addition to the influence of the algorithms' error bound and the number of iteration on the location accuracy, antenna arrangement are also key for enhanced location results. This is mostly due to the square antenna arrangement having a better spatial separation and better coverage area than the Y shaped antenna arrangement.

In Figure 7 which shows the number of PD positions located with an accuracy of 1 cm or less as a function of error bound, one may conclude that, while requiring more iterations, the SLS algorithm as applied to PD location using the square array, generally produces more accurate results than with the Y shaped array (see Figure 8).

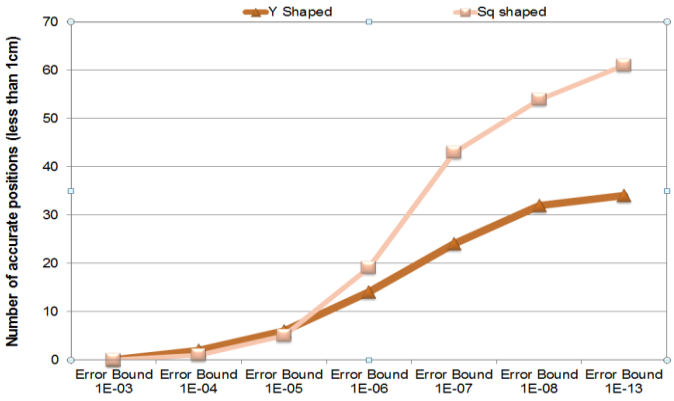

Figure 7: Number of accurate PD location solutions (< 1 cm from the PD source) for the two array configurations as a function of error bound (SLS)

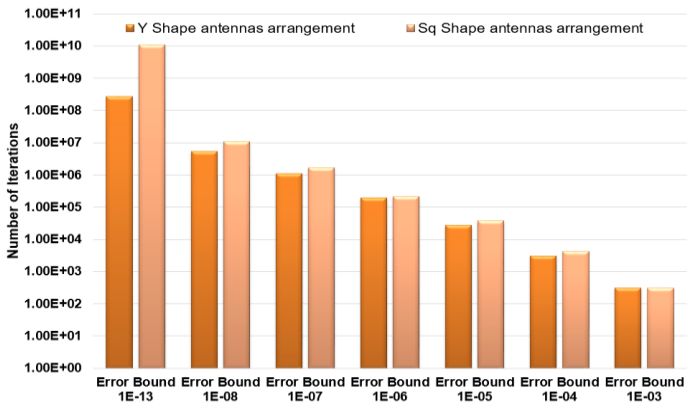

Figure 8: Number of iterations required to achieve converged solutions for each antenna configuration as a function of error bound (SLS)

4.2 Bancroft algorithm

Bancroft [21] determined a closed form expression for global positioning system pseudo-range equations. In his derivation of the formula, Bancroft made use of the Lorentz inner product and demonstrated that pseudo-range equations are hyperbolic in nature and may have two solutions. Although he did explicitly discuss the GPS navigation solution which determines the coordinates (x, y, z) and the clock offset of a GPS receiver, the understanding of the two solutions provided by the algorithm with regard to partial discharge location using RF technique is investigated in the following paragraphs.

4.2.1 Y shaped antenna array

To evaluate the performance of the two solutions provided by the Bancroft algorithm, the 64 PD positions defined on the simulation grid were computed by the Bancroft algorithm as described in Section 3. Figure 9 presents the number of correct and incorrect location solutions provided by both the positive and negative root.

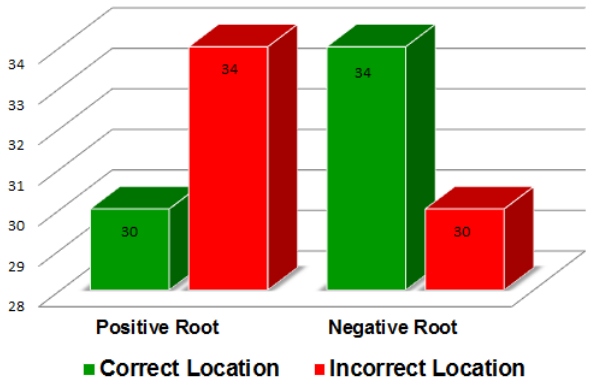

Figure 9: Location results of Bancroft algorithm using Y shaped antenna arrangement

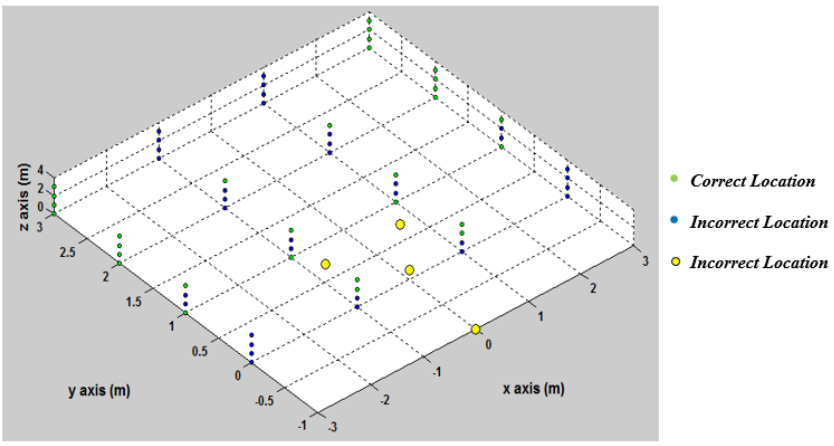

Figure 10: Position of located and non-located PD using Y shaped antenna arrangement and positive root of the Bancroft algorithm

Based on results of the positive root of the Bancroft algorithm, it can be seen that the algorithm provided accurate positioning to 30 PD locations and 34 incorrect solutions to the remaining PD positions. This demonstrates that the algorithm can only provide partial results to the 64 simulated PD using one of the roots and that the location of these simulated PD require the investigation of both solutions.

The exact position of the located and non-located PD is presented in Figure 10, where the green points represent the located positions and the blue points the incorrect solutions. It can be seen from the figure that the positioning results of located and non-located PD positions are symmetrical around the antenna central point. This is due to the topology of the Y shaped array, of which the y and z coordinates of antennas 3 and 4 are identical.

Regarding the location results of the Bancroft algorithm using the negative root, it can be seen from Figure 9 that the algorithm provided 34 accurate PD locations and 30 inaccurate PD locations. It should be noted that inaccurate locations using the positive root are found to be located accurately using the negative root and vice versa. This demonstrates that the algorithm can provide accurate locations to the 64 simulated PD

positions if valid solutions are selected between both roots. This demonstrates that the 2 solutions provided by the algorithm complement each other to provide accurate positioning to the simulated PD. This is because the two hyperbolas intersect at two locations, one that corresponds to the TDOA with correct sign and the other to the TDOA with reversed sign.

4.2.2 Square shaped antenna arrangement

Using the square antenna arrangement and the positive root, the Bancroft algorithm provided 17 correct locations and 47 incorrect locations (see Figure 11). On the other hand, positioning results using the negative root provided more accurate locations than the positive root, where 52 out of the 64 simulated PD positions located accurately and only 12 PD were located incorrectly. The difference between the correct PD locations using the positive root and the non-located PD using the negative root results from 5 PD positions being located accurately by both roots.

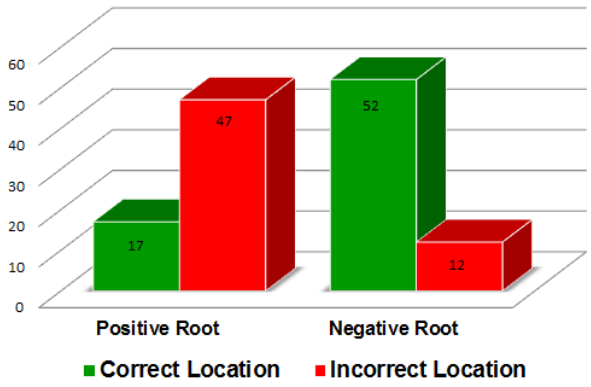

Figure 11: Location results of Bancroft algorithm using square shaped antenna arrangement

4.2.3 Discussion

Based on the results of the Bancroft algorithm using both positive and negative roots, it can be seen that the algorithm can provide very accurate location results on the 64 simulated PD positions. Results also show that the algorithm provided more successful location results when using the negative root instead of the positive root. In addition,

location results using the square antenna arrangement were found to be better than the location results when using the Y shaped antenna arrangement. Although location results using the different antenna arrangements differ in terms of the number of successfully located PD using each root, the discrimination between correct and incorrect solutions of the positive and negative root can be carried out using the clock offset parameter. Based on the simulated PD, it was found that the Bancroft algorithm can provide 100% accurate solutions to the simulated PD positions when selecting the cartesian coordinates (x, y, z) corresponding to the lowest clock offset when comparing results of both roots. Validation of this selection process may change when considering noise effects and measurement errors as time offset adjustments cannot be established due to the stochastic nature of the physical PD emission process.

Additionally, given only the difference in arrival times of the antennas' signals, it is difficult to know which solution is correct. The separation between the algorithm's correct and incorrect solutions will depend on the environment where measurements took place. For example, in the case where measurements are carried out in a high voltage power transformer using acoustic sensors attached to the transformer's housing, discrimination between the different solutions can use the equipment's area spatial volume to limit the search of valid solutions. In the case of open space areas such as electrical substations, if the reference point is at the ground height and the locations of interest are in front of the antenna arrangements, one can limit the search of valid solutions within the positive interval of y and z coordinates.

5 Comparison between Iterative and Non-Iterative Algorithms

Nonlinear equations of location algorithms which are presented by hyperbolas and distance formulas are commonly solved with iterative algorithms [26]. Results of the iterative algorithm showed that these methods have strong dependencies on different

parameters such as the error bound, number of iterations and also initial values which must be provided by the user. On the other hand, non-iterative methods, which do not require iterations and therefore make a fast computation tool, showed that they provide very accurate location results when provided by accurate TDOAs (in this case, theoretical TDOAs were provided). However the selection of correct locations among the two available solutions will depend on the user's experience and ability to discriminate between the different positioning solutions by using for example time restrictions based on the equipment's spatial volume. Table 4 presents some of the advantages and disadvantages of the different location algorithms when applied to PD location.

Table 4: Characteristics of the location algorithms

Algorithm	Advantages	Disadvantages
Iterative (SLS)	• Accurate if provided with well selected error bound • Accurate if provided with well selected number of iterations • Accurate if provided with accurate time of arrival	• Depends on number of iterations • Depends on error bound • Depends on initial values • Depends on antenna arrangement
Non-Iterative (Bancroft)	• Direct solution • Fast and very accurate • Do not depend on initial values • Possibility of discriminating between the two solutions (Bancroft method only)	• No indication of converged solutions • Depends on time of arrival accuracy • No way of discriminating between the two solutions • Provide two different solutions • Depends on antennas arrangement

Using iterative methods, the question which is still raised is: how can the user define a valid error bound and also a valid number of iterations sufficient to provide accurate location results assuming there is no initial values issue (see example of SLS performance at 10^{-13} error bound in Figure 5)?

6 New Approach

Based on simulations, it was found that when the error bound is high (e.g. 10^{-3} error bound), solutions of the location coordinates are often underestimated and the number of iterations required is also low. When the location coordinates of some TDOAs using the iterative results are compared to the location coordinates of the same TDOAs using non-iterative methods, this may show a location mismatch in the case of a non-valid error bound selection and which indicates that the error bound should be decreased. This process should be repeated until matching results are found by both iterative and non-iterative methods. Regarding the selection of a valid number of iterations, this is determined by providing enough iteration values which allow a converged solution based on the matching solutions of both iterative and non-iterative methods to be obtained. Figure 12 summarises the selection process of valid error bounds and number of iterations used by the iterative methods based on the non-iterative method solutions. It should be noted that the iterative methods may sometimes provide a non-converged solutions which may be due to initial values issue or measurement errors.

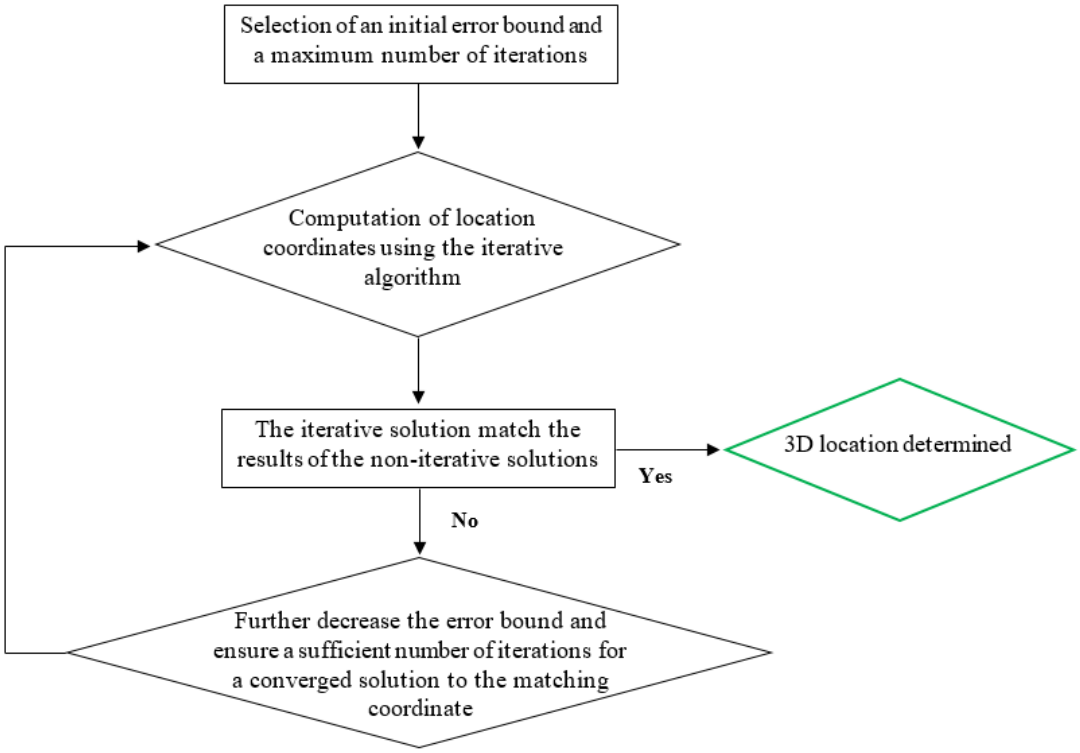

Figure 12: Selection of error bound and number of iterations

7 Conclusions

As a study evaluating the location accuracy of an iterative and non-iterative algorithms as applied to partial discharge measurement, simulations of a range of PD using two different antenna configurations have been presented.

By varying the error bounds, it has been shown that the performance of the iterative algorithms as a function of location accuracy can be quantified, despite the nonlinear nature of the location equations. A decrease in the error bound produces more accurate location results while requiring more iterations. The results presented will be useful for a practitioner of condition monitoring of in-service power equipment since it will allow judgement of appropriate levels of required accuracy based on the dimensions of the equipment under surveillance. It will also facilitate estimation of the required computing time to achieve the desired level of location accuracy. The required spatial location accuracy depends on the application. For example, general surveying of

equipment on a substation-wide scale may only require a poor to good level of accuracy (1 cm ≤ d ≤ 1 m). This range may also accurately facilitate the location of faults along large equipment sections such as busbars, bushings or power transformers (i.e. larger equipment).

Regarding the non-iterative algorithms, it was found that these techniques provide very accurate positioning when provided with precise TDOAs. The accuracy of the non-iterative algorithms also depends on the antenna arrangements which influence the number of accurate positions located by the two different roots. The discrimination process between the two different solutions of the non-iterative solutions can be difficult and will depend on the user experience to separate between the two solutions using, for example, time restrictions based on the equipment's spatial volume.

A novel approach to select adequate error bounds and number of iterations using results of the non-iterative methods has been established and will contribute considerably to solve some of the iterative method dependencies.

In this work, simulations provided an evaluation of the performance of different types of location algorithms based on determined PD locations. This evaluation method gives indications of the essential characteristics of iterative methods and also an insight on the behaviour of non-iterative methods to provide different solutions. The study presented in this paper can benefit electrical utilities, network operators and designers of PD locations systems, as it can be used as a guide to the selection of specific algorithm based on its operation requirements (i.e. computation time, discrimination between solutions, accuracy parameters and their selection process), facilitating more accurate location and diagnosis of incipient faults in high value electrical power equipment.

436 **Acknowledgements**

437 The work presented in this paper were obtained as part of a financial, academic and
438 technical support provided by Glasgow Caledonian University during the main author
439 PhD studies.

References

[1] Moore, P. J., Portugues, I. E., and Glover, I. A. “Radiometric location of partial discharge sources on energized high-voltage plant” IEEE Transactions on Power Delivery, 2005, 20, (3), pp 2264-2272

[2] Stewart, B. G., Nesbitt, A., and Hall, L. “Triangulation and 3D location estimation of RFI and partial discharge sources within a 400kV substation” Proceedings on IEEE Electrical Insulation Conference, Montreal, Canada , June 2009, pp 164-168

[3] Tian, Y., Kawada, M., and Isaka, K. “Locating partial discharge source occurring on distribution line by using FDTD and TDOA methods” IEEJ Transactions on Fundamentals and Materials, 2009, 129, (2), pp 89-96

[4] El Mountassir, O. Stewart, B, G. McMeekin, S. G. and Ahmadinia, A. “Evaluation of an iterative method used for partial discharge RF location techniques”, 10th International Conference on Environment and Electrical Engineering, 2011, pp 1-4

[5] Coenen, S. and Tenbohlen, S. “Location of PD sources in power transformers by UHF and acoustic measurements” IEEE Transactions on Dielectrics and Electrical Insulation, 2012, 19, pp 1934-1940

[6] Steiner, J. P., Reynolds, P. H., and Weeks, W. L. “Estimating the location of partial discharges in cables” IEEE Transactions on Electrical Insulation, 1992, 27, pp 44-59

[7] Tian, Y., Lewin, P., Davies, A., Sutton, S., and Swingler, S. “Partial discharge detection in cables using VHF capacitive couplers” IEEE Transactions on Dielectrics and Electrical Insulation, 2003, (10), pp 343-353

[8] Mardiana, R. and Su, C. Q. “Partial discharge location in power cables using a phase difference method” IEEE Transactions on Dielectrics and Electrical Insulation, 2010, (17), pp 1738-1746

[9] Wagenaars, P., Wouters, P. A. A. F., Van der Wielen, P. C. J. M., and Steennis, F. “Influence of ring main units and substations on online partial discharge detection and location in medium voltage cable networks” IEEE Transactions on Power Delivery,2011, (26), pp 1064-1071

[10] Meijer, S., Smit, J. J. and Girodet, A. “Estimation of UHF signal propagation through GIS for sensitive PD detection” IEEE International Symposium on Electrical Insulation, 2002, pp 435-438

[11] Hu, X., Judd, M. D., and Siew, W. H. “A study of PD location issues in GIS using FDTD simulation”. International Universities Power Engineering Conference, 2010, pp 1-5

[12] Hikita, M., Ohtsuka, S., Wada, J., Okabe, S., Hoshino, T., and Maruyama, S. “Study of partial discharge radiated electromagnetic wave propagation characteristics in an actual 154kV model GIS” IEEE Transactions on Dielectrics and Electrical Insulation, 2012, (19), pp 8-17

[13] Chiu, M. Y., Liang, K.W., Lee, C. H., Fan, C. L., Cheng, J., and C., L. Y. “Application of MV GIS partial discharge measurement and location” International Conference on Condition Monitoring and Diagnosis, 2012, pp 462-465

[14] Zheng, B and Bojovschi, A. “Electromagnetic Sensing of Partial Discharge in Air-insulated Medium Voltage Switchgear”, IEEE Power Engineering and Automation Conference, 2012, pp 1-4

[15] Judd, M. D., Yang, L., and Hunter, I. B. B. “Partial discharge monitoring for power transformer using UHF sensors. Part 2: Field experience” IEEE Electrical Insulation Magazine, 2005, (21), pp 5-13

[16] Tang, Z. G., Chengrong, L. R., Xu, C. ; Wei, W., Jinzhong, L., and Jun, L. “Partial discharge location in power transformers using wideband RF detection” IEEE Transactions on Dielectrics and Electrical Insulation, 2006, (13), pp 1193-1199

[17] Sinaga, H. H., Phung, B. T., and Blackburn, T. R. “Partial discharge localization in transformers using UHF detection method” IEEE Transactions on Dielectrics and Electrical Insulation, 2012, (19), pp 1891-1900

[18] Zhang, X., Tang, J., and Xie, Y. “Taylor-genetic algorithm on PD location” International Conference on High Voltage Engineering and Application, 2008, pp 685-688

[19] Miao, P., Li, X., Huijuan, H., Gehao, S., Hu, Y., and Jiang, X. “Location algorithm for partial discharge based on radio frequency (RF) antenna array” Asia-Pacific Power and Energy Engineering Conference, 2012, pp 1-4

[20] Y. Lu, X. Tan, X. Hu, “PD detection and localisation by acoustic measurements in an oil-filled transformer”, IEEE Transactions on Science, Measurement and Technology, 2002, (147), pp 81-85

[21] O. El Mountassir, B. G. Stewart, S. G. McMeekin and A. Ahmadinia. “Effect of sampling rate on the location accuracy of measurements from radiated RF partial discharges signals” 11th International Conference on Environment and Electrical Engineering, 2011, pp 891-896

[22] Bancroft, S. “An algebraic solution of the GPS equations” IEEE Transactions on Aerospace and Electronic Systems, 1985, (21), pp 56-59

513 [23] Ho, K. M. and Chan, Y. T. “Solution and performance analysis of geolocation
514 by TDOA” IEEE Transactions on Aerospace and Electronic Systems, 1993,
515 (29), pp 1311-1322
516 [24] Yang, M. and Chen, K. H. “Performance assessment of a noniterative algorithm
517 for global positioning system (GPS) absolute positioning” Procceedings of the
518 National Science Council, 2001, (25), pp 102-106
519 [25] Bucher, R. and Misra, D. “A synthesizable VHDL model of the exact solution
520 for three-dimensional hyperbolic positioning system” VLSI Design Journal,
521 2002, (15), pp 507-520
522 [26] Markalous, S., Tenbohlen, S., and Feser, K. “Detection and location of partial
523 discharges in power transformers using acoustic and electromagnetic signals”
524 IEEE Transactions on Dielectrics and Electrical Insulation, 2008, (15), pp 1576-
525 1583